Automated Sea Ice Concentration Analysis History at NCEP

1996-2012

Robert W. Grumbine *

Marine Modeling and Analysis Branch, EMC/NCEP/NWS/NOAA

* *Corresponding author address:* Robert W. Grumbine, NCWCP (W/NP21) 5830 University Research Ct., College Park, MD 20740.

E-mail: Robert.Grumbine@noaa.gov

ABSTRACT

In the years since the first implementation of sea ice concentration analysis, the analysis system has evolved. While the basics remain the same, there have been many changes in details – weather filtering, which instruments are used, how they are used, land masks, and so forth have all changed somewhat or very much. This note documents the evolution of the system from 1996, when the original note was published, until 2012, the date of the last major changes to the system.

List of Acronyms

AMSR-E	Advanced Microwave Scanning Radiometer
BUFR	Binary Universal Form for Representation of Meteorological Data
CAFTI	Committee Assessment of Forecast Technique Improvement
CFS	Climate Forecast System
CFSRR	Climate Forecast System Reanalysis and Reforecast
CIS	Canadian Ice Service
DMSP	Defense Meteorological Satellite Program
EMC	Environmental Modelling Center
EOS	Earth Observing System
ERS	European Remote Sensing Satellite
FNMOC	Fleet Numerical Meteorology and Oceanography Center
GFS	Global Forecast System (successor to MRF)
GRIB	Gridded Binary – WMO standard for exchange of gridded fields
GTS	Global Telecommunication System
HDF	Hierarchal Data format – EOS standard for exchange of gridded fields
ISLSCP	International Land Surface Climatology Project
MMAB	Marine Modeling and Analysis Branch (successor to OMB)
MRF	Medium Range Forecast (succeeded by GFS)
NARR	North American Reanalysis and Reforecast
NASA	National Aeronautics and Space Administration
NCAR	National Center for Atmospheric Research
NCEP	National Centers for Environmental Prediction
NESDIS	National Environmental Satellite Data Information Service
NIC	National Ice Center
NOAA	National Oceanic and Atmospheric Administration
NSIDC	National Snow and Ice Data Center
NWS	National Weather Service

OI	Optimal Interpolation
OMB	Ocean Modelling Branch
RTG	Real-Time, Global
SDR	Satellite Data Record
SMMR	Scanning Multichannel Microwave Radiometer
SSMI	Special Sensor Microwave/ Imager
SSMI-S	Special Sensor Microwave/ Imager - Sounder
SST	Sea Surface Temperature
WMO	World Meteorological Organization

1. Introduction

The original operational automated sea ice analysis system was documented in (Grumbine 1996). Much has changed since then, and this document will describe the current operational system (as of 19 June 2012) with some reference to changes which occurred in the interim.

The automated sea ice analysis is important within the National Centers for Environmental Prediction (NCEP) because models and other analysis systems require information about the ice cover in order to do their work. This includes the Global Forecast System (GFS) (Lord et al. 2007), WAVEWATCH III(tm) wave model (Tolman 1991; Tolman et al. 2002), Climate Forecast System (CFS) (NCEP/EMC/GCWMB 2011), and sea surface temperature analysis systems (1 degree OI (Reynolds and Smith 1994), quarter degree OI (Reynolds et al. 2007), RTG low and high resolution (Thiebaux et al. 2003; Gemmill et al. 2007). Further, much use is made by other groups, including within NESDIS for sea surface temperature analysis (Reynolds et al. 2002).

Given the purpose of NWS, the best possible forecasts, and best possible forecast guidance, algorithms and data sources have been chosen to that end. A consequence is that as either changes, users more concerned with climate will see some discontinuities, e.g. (Screen 2011).

2. Satellite History

In order to produce an analysis automatically, it is important to use information which is available day or night, as the polar night is 6 months long, and which can be used in the presence of clouds, as the polar regions are often cloudy (Huschke 1969).

Visible wavelengths are, therefore, not as desirable as microwave because of both night and cloud concerns. Even infrared is questionable, due to cloud concerns. Though work is in progress to develop algorithms which address this (starting with, e.g., Emery and Fowler in (Cavalieri et al. 1992)). Microwaves, on the other hand, pass readily through clouds and are emitted from the surface regardless of day/night concerns. Instruments which have been available in NCEP operations include the SSMI and AMSR-E. SSMI-S from the DMSP F-16, F-17, and F-18 are now available, but current algorithms in NCEP cannot be applied unmodified to F-16 and F-18 SSMI-S, as their observations are discrepant from F-17's. Work is proceeding to develop and implement the needed modifications.

Table 1 provides the listing of satellites which have been available (and their dates), and the dates during which they were actually used in NCEP operations or pre-operations.

3. Satellite Algorithms

Original Implementation

The original implementation used the NASA Team Algorithm (Cavalieri et al. 1992). This algorithm uses observations from 19 GHz (horizontal and vertical polarization – H and V) and 37 GHz (H and V) to compute the sea ice concentration. Weather filtering (more in next section) is done using 22 GHz V, 37 GHz V, and 19 GHz V. This algorithm was as good as any and better than most when originally implemented operationally in NCEP in 1997 (e.g. see analysis by (Andersen 2000)).

There was, however, concern about low bias to sea ice concentrations in the Antarctic.

Consequently, the NASA Team2 algorithm was developed (Markus and Cavalieri 2000). This had little effect on sea ice extent computations, but sea ice area was increased by several percent over the southern hemisphere ((Screen 2011) for some issues).

Table 2 gives the listing of dates for when and which algorithms were in use.

NCEP Modified high resolution algorithm

This algorithm was developed in 2000-2001 in response to requests for higher resolution sea ice analysis. At that time, the instrument in use was the SSMI. The Team 1 concentration algorithm uses information from 19 GHz channels, which have a footprint of approximately 50 km radius (Cavalieri et al. 1992). Though data are reported from the instrument every 25 km, which was the grid spacing of the analysis (25.4 km), the reality of the 50 km footprint is easily seen in the smoothness of analyzed concentration fields, and in the great distance from shore to which land contamination could be seen. Among other things, this rendered it impossible to analyze ice concentrations over large inland water bodies like Great Slave Lake.

Therefore, this modification was to use only information from the highest resolution channels from the SSMI – the 85 GHz channels (V + H polarization), which had a footprint of about 12.7 km. Consequently a new analysis grid, of 12.7 km resolution, was implemented (the August, 2004 implementation), with the modified algorithm.

The principles used in developing the modification were that the new version could use only 85 GHz, so as to retain highest possible resolution, and it had to remain very near the analysis given by the reference algorithm (Team 1 to August 2006, Team2 since then, for SSMI use). A number of candidate parameters were tried. The parameter which gave the best results, in linear regression against the reference algorithm, in areas the reference can be expected to be most reliable, was one of the Stokes' parameters for polarized radiation – sqrt($T85V^2$ - $T85H^2$). Correlations are always in excess of 0.9 with the Team1 reference. Since the higher resolution is seeing more detail, we do not expect perfect correlation.

Let H represent the brightness temperature at 85 GHz horizontal polarization, and V be brightness temperature at 85 GHz vertical polarization. Trial functions were:

```
H
V
V-H
V+H
V/H
V*H
V*V
H*H
V*(V-H)
(V-H)/V
(V+H)/V
(V-H)*(V+H) -> V^2 - H^2
sqrt(V^2 - H^2)
```

The points where the reference algorithm is computed, to have a basis to estimate the day's regression parameters for the sea ice cover, are points poleward of 60 degrees, and which are more than 100 km from land (the approximate range of land contamination).

Figures 1 and 2 show the Arctic and Antarctic changes in area and extent when changing the AMSRE lookup tables from the operational to planned for operational implementation (pre-launch table vs. latest table [Cavalieri and Markus, personal communication, 2010]). Area is much more sensitive than extent. Area is the area of ice on the ocean. Extent is computed in grid cells – the total area of any grid cell with any ice is added for extent. Extent is therefore always larger than area.

Table 2 gives the dates of each algorithm which was used in operations. Some additional dates regarding the operational analysis system are:

March 1996 – Approved for operational implementation by CAFTI

September 1997 – Original Operational Implementation

February 1998 – Used in global atmospheric model

September 1999 – Cray fire

4. Filtering and Quality Control

a. Coarse Quality Control

Prior to attempting to use the weather filters for the sea ice concentration algorithm, coarse quality control bounds are applied. These apply to the brightness temperatures themselves, but also the locations and surface flags. Limits are given in Table 3. If any data on a scan (SSMI, AMSR-E) or spot (SSMI-S) are bad, then the entire scan is declared 'bad' and it is ignored. Source code for this is in file process_bufr.C. Also H > V is considered bad.

b. Weather filtering on the grid

The traditional weather filter used for the NASA Team and NASA Team2 (Gloersen and Cavalieri 1986) algorithms is overloaded, in the sense that it is used both to indicate areas that do not have sea ice, and areas where it might appear that there is sea ice, but the sensor data have been corrupted by weather.

In this weather filter, we aim to separate the two functions. This will lead to 3 outcomes for the filter – 'ocean', 'ice' (thence to compute the ice concentration using the ice concentration algorithm), and 'weather'. 'weather' will now mean solely that the brightness temperatures might be resulting from active weather systems. Separate from that, there will be a flag for ocean directly from the filter. This is useful in the automated sea ice concentration processing because 'weather' is considered a non-observation. After a sufficiently long period of no observations, concentrations are set to zero (Grumbine 1996). With

changes from a strictly SSMI-based ice concentration system to one including the somewhat different AMSR-E channels and filters, areas of sea ice are now being flagged as 'weather' for extended periods – long enough to run in to this processing limit. With a flag devoted to setting concentrations to zero when and where we are confident that they are, in fact, zero, the age-based processing can be examined on its own and, hopefully, be tuned to methods more appropriate to the newer instrument.

There are a number of candidate functions to test – critical temperature type functions (T >T_*crit*, or T < T_*crit*), polarization ratio (T_v - T_h)/(T_v+T_h), and gradient ratio (T_*i*-T_*j*)/(T_*i*+T_*j*). The NASA Team and Team2 weather filter (Gloersen and Cavalieri 1986) uses 0.045 as the limit for gradient ratio of 22 V to 19 V, and 0.05 for GR37LIM. For the exhaustive search, I take the observed range of each function, split that in to 256 steps, and evaluate the performance of each step.

There are three competing criteria for a good filter. It should never flag an observation as ocean unless it truly is not ice (flagging 'ocean' over a land point is acceptable) (high probability of detection, with low false alarm rate). It should only flag 'ice' over points that truly are ice (again, high probability of detection with low false alarm rate). And it should seldom flag points as weather (straight frequency should be low). This is, therefore, a problem of multiobjective optimization (see discussion in, for example, (Eiben and Smith 2003)).

The resultant filter is:

```
If both water and ice filter are triggered: Weather Flag
  else:
Water Flag: if (T19V - T19H) / (T19V + T19H) > -0.055  -> water
  Ice Flag: if (T19V - T87V) / (T19V + T87V) > +0.2412 -> ice

If Ice Flag: compute sea ice concentration
```

c. *A Posteriori filtering*

It is common for sea surface temperature analyses (e.g. (Reynolds and Smith 1994; Reynolds et al. 2007; Thiebaux et al. 2003; Gemmill et al. 2007)) to use sea ice concentration in their procedures. It is also common (Grumbine 1996; Fetterer et al. 2002, updated 2009; editor) for sea ice concentration analyses to use sea surface temperature. This presents a possibility for an 'incestuous' feedback, wherein a too-cold SST permits a point which the weather filter failed to remove to become analyzed as ice. Then, since the ice analysis identifies a point as ice, the next SST analysis uses that 'observation' to retain or cool even further the water point. Such a feedback seldom occurs in practice, but it did do so in the high resolution RTG analysis in summer of 2007 [R. Grumbine, personal observation].

To reduce the possibilities for this feedback, an *A Posteriori* filter was developed (Grumbine 2009) and started in use for the CFSRR (Saha et al. 2010) and operational implementation in October, 2011. This is still based on SST, but on climatological SST – any point which has never been observed (in the (Reynolds et al. 2007), from 1984-2009) to be warmer than the critical temperature (275.3) is always masked out of the sea ice analysis. This does leave the possibility for the feedback, but experience shows that the weather filter is most effective in the colder near-ice ocean than farther away. The area that did experience the feedback in 2007 was the east coast of Japan.

d. *SST filtering*

Finally, the ice analysis is filtered against the current SST analysis. Water warmer than 275.3 K is deemed incapable of having an ice cover, as was the case in (Grumbine 1996). The source, however, of the SST has changed through time. The original SST (1994-26 August 2004) was the daily 1 degree OI (Reynolds and Smith 1994). This was changed to the low resolution (half degree) Real Time Global (RTG) SST (Thiebaux et al. 2003), through 10 August 2006. And the high resolution RTG (1/12th degree) SST (Gemmill et al. 2007) 11

August 2006 to present.

With the new (2010) *A Posteriori* filtering, the SST filter mainly affects only inland water bodies that are not analyzed in OIv2 (Reynolds et al. 2007).

5. Gridding

a. Earth Mapping

The high resolution grid is 12.7 km on the polar stereographic "analyst's" grid, originally 25.4 km. The earth's equatorial radius is 6378.160 km, and its $eccen^2 = 0.006694604$. True at 60 N or S. Latitudes and longitudes are computed by (Troisi 1994), and represent the center of grid cells.

The high resolution latitude-longitude "modeller's" grid is 5 arcminutes, the low resolution grid is 30 arcminutes.

b. Land Masking

The land masks themselves were originally derived from a NESDIS land mask at 1/16th degree (approximately 7 km) resolution (Grumbine 1996). This was good resolution for the 30' latitude-longitude files, and reasonable for the 25.4 km polar stereographic grids. It is not as well-suited to the higher resolution files at 12.7 km polar stereographic and 5' (1/12th degree) latitude-longitude. For this reason in the high resolution implementation of 2004, though the land mask was initially derived from this data set as before, points which were not entirely land-flagged (that is, not all the NESDIS points which would map into the given grid cell were land) were left water for later analysis. The later analysis was to examine those points which were near the land-flagged points, and which retained an 'ice cover' through July-August in the northern hemisphere (away from places, like Hudson Bay, which might have real ice covers in part of that time). Since land betrays a sea ice signature, and we

know that there's no sea ice in, say, the Aral Sea during August, this permits a more suitable land mask to be developed even without having higher resolution data sources to draw from. It also permitted us, as was known to be needed for the Aral Sea, to produce a land mask which is appropriate to the current boundaries of lakes and coasts when lakes dry up or ice shelves calve ice bergs (such as B-9 (Keys et al. 1990)) which are larger than the grid resolution.

The drawback is that the NESDIS land mask itself erred on the side of flagging points as land, and this process will tend to err even farther in that direction due to the footprint (12.7 km) of the sensor used. Consequently, many lakes which are, in principle, large enough to be resolved by the grid were left flagged as land. Nevertheless values in the lakes, such as Baikal, Great Bear, Great Slave, which were considered resolvable could be used with much more confidence.

For the current land masks, implemented operationally in August, 2008, two different high resolution data sources were examined. One is a 0.5' land mask from (Hansen et al. 2000). The other is a coastline data file with spacings as fine as 200 m (Wessel and Smith 1996). With data sources this fine, the sea ice grids are coarse, and it is relatively easy to decide mask values. For this generation of land masks, the basic (previously the only) land mask is aimed at greatest geographic faithfulness, with no allowances for satellite sensors and their foibles. The 5' and 12.7 km land masks are derived from the 0.5' land mask in the same algorithm as from the original 3.75'. They are derived from the coastline files by examining, grid point by grid point, whether the bounding polygon passes through the grid cell (leading to a 'coast' flag), or the point is inside or outside the bounding curve (land flag if inside a land polygon, etc.). Coast points are then resolved to land or water depending on bathymetry/topography, and bathymetry/topography files are generated as well. For more detail on this aspect, see (Grumbine 2012).

The land masks generated from those two data sets are quite similar, as would be hoped. They do differ, though. The largest differences are in the ice shelf regions of Antarctica,

where the 0.5' mask (Hansen et al. 2000) leaves these points as water, while the coastline files (Wessel and Smith 1996) consider them as land. For the purpose of performing ocean surface analysis and modelling, ice shelves are more reasonably considered to be land so we follow the coastline file. In the northern hemisphere, the differences are small. As I will be using the shoreline curves in conducting my analysis procedures (sections Gridding Ice Concentrations, and Inland Water Bodies), I use the land mask derived from them in the northern hemisphere, too.

Both sources (Hansen et al. 2000; Wessel and Smith 1996) consider the Aral Sea to have its mid-20th century size, which leaves a less than ideal grid.

Since the global analysis product is derived from the polar stereographic hemispheric analyses, one further step is made. It was realized in developing sea ice cover for the North American Regional Reanalysis (Mesinger et al. 2006) that there could be points on the target grid which could not be filled directly from source information grids. This does not happen with the current 5' and 12.7 km grids. But it is a point which must be verified with each future update to the masks.

c. Filling the Grids

Each observation from the satellite is mapped against the polar stereographic grid and added in a 'drop in the bucket' sense, as in (Grumbine 1996). The sea ice concentration (or weather flag, as the case may be) is added to, and only to, the grid cell which is closest to the observation's location. If there are multiple valid observations, the concentration is the average of them. But if more than 1/3rd of the observations in a grid cell are 'weather', it is flagged 'weather'.

The global grid is filled from the polar stereographic, again in drop in the bucket sense. Each grid point in the polar stereographic is added to the nearest global grid point. There are no points on the global grid which do not receive information from at least 1 grid point on the polar stereographic grid. If multiple polar stereographic grid cells contribute to a

global grid, the concentrations (valid ice concentrations only) are averaged.

6. Reanalysis Fields

Sea ice concentrations have been an important part of reanalysis efforts, including the NCEP/NCAR Reanalysis (Kalnay et al. 1996), the North American Regional Reanalysis (Mesinger et al. 2006), and the Climate Forecast System Reanalysis and Reforecast (Saha et al. 2010). Each of these reanalyses has made use to some degree of the then-operational approach to sea ice concentration analysis. A separate document will discuss each of these in detail. Also see (Sellers et al. 1996) for the ISLSCP-I ice, mentioned in (Grumbine 1996).

A fundamental question in constructing any reanalysis sea ice cover is whether it is more important to provide greatest stability in the ice treatment, or to provide the best estimates possible at the time of the reanalysis, and for the dates of reanalysis. In these three, the emphasis was placed on best possible fields, which does introduce some artefacts in the time series such as sudden increase in Antarctic sea ice area (though not extent) when the Team2 algorithm was implemented (Screen 2011).

7. Distribution

The low resolution grids, both polar stereographic and latitude-longitude, are distributed via GTS as KWBM OEXA88, OENA88, and OESA88 for global latitude-longitude, northern hemisphere, and southern hemisphere, respectively.

Nonoperational web and ftp distribution has been available since October 1995, at `http://polar.ncep.noaa.gov/seaice/Analyses.html` (original name polar.wwb.noaa.gov). Animations of the most recent 30 days were added to the web site in December 1999. A climatological reference was included July 2002 based on (Chapman and Walsh 1991) at `http://polar.ncep.noaa.gov/seaice/Historical.html` along with saved monthly ani-

mations. A newer climatology, based on the CFSRR sea ice, is in preparation.

Operational ftp distribution of the current day's analysis is available at
`ftp://ftpprd.ncep.noaa.gov/pub/data/nccf/com/omb/prod/sice.YYYYMMDD`
where YYYYMMDD is the 8 digit year, month, day group.

There is currently no official NOAA archival site for these analyses. They are available non-operationally at `ftp://polar.ncep.noaa.gov/cdas/archive` for the global grids, and `ftp://polar.ncep.noaa.gov/ice/archive` for the hemispheric grids. These extend back to the October, 1995 inauguration of the web site, but with some gaps due to its non-operational status. The files are of the data as processed on that day, so there are the discontinuities in content.

ISLSCP 1 sea ice fields are at `ftp://polar.ncep.noaa.gov/history/islscp1`

Reanalysis 1 sea ice fields are at
`ftp://polar.ncep.noaa.gov/history/ice/reanl.ice/`

NARR sea ice fields are at `ftp://polar.ncep.noaa.gov/history/ice/narr/`

CFSRR sea ice fields are at `ftp://polar.ncep.noaa.gov/history/ice/cfsrr/`

Each has greatest continuity of method up to the date of original implementation, and follows what was operational (`ftp://polar.ncep.noaa.gov/cdas/`) thereafter. More detail on reanalysis sea ice concentrations will follow in individual technical notes.

8. Conclusions

Maintaining and improving a sea ice concentration analysis system requires regular updates to the system as satellites age, improved algorithms are developed, new satellites come on line, and user needs expand. This document describes the moving target that has been the operational sea ice concentration analysis system at NCEP for the past 16 years of its operations. Further modifcations will occur now that SSMI-S is being used, and AMSR-2 will soon be providing data. The next document will not be 16 years in the making!

While we are primarily concerned with sea ice concentrations for use on weather time scales, whether by atmospheric, oceanic, or ice models, the multiple experiences at developing ice fields for use in weather and climate reanalyses have pointed to a number of features useful to even the weather analysis system. This includes the a posteriori ice filter, and obtaining ice concentrations at points outside the analysis grid by correlation to points inside the grid, or concentrations in areas which are unobserved for extended periods by such correlation.

Acknowledgments.

I would like to thank the many people who have helped improve the sea ice concentration analysis system, including but not only: Diane Stokes, Bert Katz, Xingren Wu, William H. Gemmill, Hendrik Tolman – NCEP, Richard Reynolds, Viva Brazon, Chunying Liu NCDC, Donald J. Cavalieri and Thorsten Markus NASA GSFC, Julienne Stroeve, Mark Serreze NSIDC

REFERENCES

Andersen, S., 2000: *Evaluation of SSM/I sea ice algorithms for use in the SAF on ocean and sea ice*, Vol. CO-10. Danish meteorological insitute scientific report, 49 pp.

Cavalieri, D. J., et al., 1992: *NASA Sea Ice Validation Program for the DMSP SSM/I: Final Report. NASA Technical Memorandum 104559.* National Aeronautics and Space Administration, Washington, DC, 126 pages.

Chapman, W. L. and J. E. Walsh, 1991: Long-range prediction of regional sea ice anomalies in the arctic. *Weather and Forecasting*, **6**, 271–288.

(editor), S. E., 2012: Ocean & sea ice saf sea ice product manual version 3.8. OSISAF.

Eiben, A. E. and J. E. Smith, 2003: *Introduction to Evolutionary Computing*. Springer-Verlag, Berlin, 299 pp.

Fetterer, F., K. Knowles, W. Meier, and M. Savoie, 2002, updated 2009: Sea ice index. National Snow and Ice Data Center, digital media., digital media.

Gemmill, W., B. Katz, and X. Li, 2007: Daily real-time global sea surface temperature - high resolution analysis at NOAA/NCEP. Tech. rep., MMAB. NOAA / NWS / NCEP / MMAB Technical Note Nr. 260, 39 pp.

Gloersen, P. and D. J. Cavalieri, 1986: Reduction of weather effects in the calculation of sea ice concentration from microwave radiances. *J. Geophys. Res.*, **91 (C3)**, 3913–3919.

Grumbine, R. W., 1996: Automated sea ice concentration analysis. *MMAB Technical Note*, **120**, 13.

Grumbine, R. W., 2009: *A posteriori* filtering of sea ice concentrations. Tech. rep., MMAB. NOAA/NWS/NCEP/MMAB Technical Note 282, 8 pp.

Grumbine, R. W., 2012: Automatic generation of land masks and bathymetry for satellite analysis and model use. Tech. rep., MMAB. NOAA/NWS/NCEP/MMAB Technical Note 301, NN pp.

Hansen, M., R. DeFries, J. Townshend, and R. Sohlberg, 2000: Global land cover classification at 1km resolution using a decision tree classifier. *International Journal of Remote Sensing*, **21**, 1331–1365, data Source: Global Land Cover Facility (GLCF) at www.landcover.org.

Huschke, R. E., 1969: *Arctic Cloud Statistics from 'Air-Calibrated' Surface Weather Observations*. Rand Corporation, Santa Monica, CA, 79 pp.

Kalnay, E., et al., 1996: The NCEP/NCAR 40 year reanalysis project. *Bulletin of the American Meteorological Society*, **77**, 437–471.

Keys, H., S. S. Jacobs, and D. Barnett, 1990: The calving and drift of iceberg B-9 in the Ross Sea, Antarctica. *Antarctic Science*, **2**, 243–257.

Lord, S., J. Derber, M. Iredell, R. Treadon, W.-S. Wu, D. Parrish, and D. Kleist, 2007: NCEP satellite data assimilation overview, 1 May 2007. NCEP/EMC, unpublished, unpublished.

Markus, T. and D. J. Cavalieri, 2000: An enhancement of the NASA Team sea ice algorithm. *IEEE Trans. Geosci. Remote Sens.*, **38**, 1387–1398.

Mesinger, F., et al., 2006: North american regional reanalysis. *Bulletin of the American Meteorological Society*, **87**, 343–360, doi: 10.1175/BAMS-87-3-343.

NCEP, 2012: bufrlib. NCEP, http://www.nco.ncep.noaa.gov/sib/decoders/BUFRLIB/, http://www.nco.ncep.noaa.gov/sib/decoders/BUFRLIB/.

NCEP/EMC/GCWMB, 2011: CFS v2.0. NCEP/EMC.

Reynolds, R. W., N. A. Rayner, T. M. Smith, D. C. Stokes, and W. Wang, 2002: An improved in situ and satellite SST analysis for climate. *J. Climate*, **15**, 1609–1625.

Reynolds, R. W. and T. M. Smith, 1994: Improved global sea surface temperature analysis using optimal interpolation. *J. Climate*, **7**, 929–948.

Reynolds, R. W., T. M. Smith, C. Liu, D. B. Chelton, K. S. Casey, and M. G. Schlax, 2007: Daily high-resolution-blended analyses for sea surface temperature. *J. Climate*, **20**, 5473–5496.

Saha, S., et al., 2010: The NCEP climate forecast system reanalysis. *Bulletin of the American Meteorological Society*, **91**, 1015–1057, doi: 10.1175/2010BAMS3001.1.

Screen, J. A., 2011: Sudden increase in antarctic sea ice: Fact or artifact? *Geophysical Research Letters*, **38**, http://dx.doi.org/10.1029/2011GL047553.

Sellers, P., et al., 1996: International satellite land surface climatology project - initiative i data collection (islscp i), [internet]. NASA distributed active archive center (daac). National Aeronautics and Space Administration, Goddard Space Flight Center, http://badc.nerc.ac.uk/view/badc.nerc.ac.uk__ATOM__dataent_ISLSCP, http://badc.nerc.ac.uk/view/badc.nerc.ac.uk__ATOM__dataent_ISLSCP.

Thiebaux, H. J., E. Rogers, W. Wang, and B. Katz, 2003: A new high-resolution blended real-time global sea surface temperature analysis. *Bulletin of the American Meteorological Society*, **84**, 645–656.

Tolman, H. L., 1991: A third-generation model for wind waves on slowly varying, unsteady and inhomogeneous depths and currents. *J. Phys. Oceanography*, **21**, 782–797.

Tolman, H. L., B. Balasubramaniyan, L. D. Burroughs, D. V. Chalikov, Y. Y. Chao, H. S.

384 Chen, and V. M. Gerald, 2002: Development and implementation of a wind-generated
385 ocean surface wave models at NCEP. *Weather and Forecasting*, **17**, 311–333.

386 Troisi, V., 1994: mapll.f and mapxy.f. NSIDC.

387 Wessel, P. and W. Smith, 1996: A global self-consistent hierarchical high-resolution shoreline
388 database. *J. Geophys. Res.*, **101(B4)**, 8741–8743.

389 Woolen, J., 2012: dumpjb. NCEP/EMC.

APPENDIX A

Source Code Evolution

a. Programs Involved

The job which controls the analysis is formerly J990, then named JMRF_ICEDRFT2.sms.prod, and, with the 19 June 2012 implementation, JSEAICE_CONCENTRATION_ANALYSIS. This then invokes script ex990 (then exmrf_icedrft2.sh.sms, now exseaice_concentration_analysis.sh.sms).

External to the sea ice processing itself are the bufrlib (NCEP 2012) and dumpjb (Woolen 2012), which are used to extract data from the NCEP operational BUFR tanks. 24 hours of data centered on 00 UTC are requested, the analysis being for 00 UTC of the given day, and a daily average. The run time of the program is 11:30 UTC, which means data are biased slightly earlier than the nominal 00 UTC center.

The first program of the automated processing proper is seaice_ssmibufr, which extracts data from the full bufr tank form and format and rewrites it to something more convenient to the sea ice processing. Each instrument type has a corresponding program of this type – seaice_amsrbufr, seaice_ssmisbufr. The original amsr decoder only used locations from the low frequency channels. Loss of the instrument's data in October 2011 prevented an implementation using the high resolution channels' individual locations. Original ssmibufr only used low resolution channels' locations. The 2004 implementation used high resolution locations, repeating the low resolution channel information for each high resolution location.

Program seaice_seaissmi then constructs the high resolution sea ice analysis grids, northern and southern hemispheres, for a given satellite (now, originally only for F-13, then for all ssmi data it was given). This permits the option of producing separate grids for each satellite and then combining or assimilating them.

If more than one instrument type is available, this pairing of debufr/analyze is and will be repeated for each of them. Hence there was seaice_amsbufr and seaice_seaiamsr, and will be seaice_ssmisbufr and seaice_seaissmis.

Next, the analyst grids from each instrument type are blended together in program seaice_blend. The current approach is to treat all sources as equal, and use arithmetic averages when more than one instrument is available, and use the one instrument's output if only one is available. Since the 16 June 2012 implementation, 3 instruments are used – (F-15, AMSR-E, F-17 – even though AMSR-E is not providing data, its grid of 'no data' is ingested. In the future, AMSR2 will provide data, and this space will then be used.)

A preliminary coarse filter is applied to these grids to prevent areas from being falsely treated as sea ice. This is program seaice_posteriori, which uses a climatologically-based grid of coldest ever-observed temperatures to filter out points which have not been observed to be colder than 275.3 K (the cutoff used in seaice_filtanal below). Full description is in (Grumbine 2009).

To preserve the original 25.4 km output, which is also sent over GTS – unlike the 12.7 km output – these higher resolution grids are downscaled by program seaice_reduce (seaice_north_reduce and seaice_south_reduce, but the source code is identical – grid selection is a compile-time option). The downscaling algorithm is to average all valid ice concentrations in the 4 cells of the 12.7 km grid on to the corresponding cell of the 25.4 km grid. Since even 1 water point on the 12.7 km grid will give a concentration on the 25.4, this produces significantly more extensive lakes and bays on the 25.4 km grid than geography would expect. Its virtue and reason is that if a downstream user has a somewhat different land mask at 25 km than is derived in NCEP, they will still (probably) have a valid ice concentration. The first modification was to put land flags directly in the output for points which have no valid high resolution concentration. Land flags have also been put in the half degree sea ice concentration analysis since 27 August 2004.

For quality control purposes, seaice_toxpm is also run on the data, to produce xpm

graphic files which are then converted to png or gif and placed on web service. (Again, separate executables for each area and resolution, but only 1 source.) When seaice_reduce started putting land flags on unfillable points, for the polar stereographic grids this also meant unfillable because of having no data. For graphic consistency, seaice_toxpm was then modified to show 'no data' on points that could not be filled and were not land in the land mask file. The original color bar was an ugly scientist-derived bar. National Geographic [personal communication, 1996] provided the bar that has been used since 1996. (See Nat Geo May, 1996 for illustration.)

The binary output is converted to grib and GTS formatted files produced in seaice_psg. (Mnemonic being polar stereographic grid.)

System utilities cnvgrib and wgrib2 were used until 16 June 2012 to construct grib2 output from native grib1 output of seaice_psg. Program seaice_grib2 generates grib2 files for all resolutions and projections. Input files seaice_pds and gds.(grid) provide the grid specification information to grib2. The original program was provided by Vera Gerald [personal communication, 2011].

This concludes construction of the polar stereographic grids, which are oriented to 'sea ice analysts' – people who understand the nature of the data, can accept data gaps (due to no clear observation, or simply that the orbital passes did not cover an area), and can accept false positives for ice. (The algorithm is not perfect, nor is the weather filtering in the seaice_seaissmi program, so some points which are certainly not sea ice are nevertheless called ice in these grids.)

For users who need complete coverage each day, and cannot afford those false ice points, such as weather, wave, and ocean modellers, a global latitude-longitude grid at 5' resolution is constructed. And from that, a 30' grid.

The most recent high resolution real-time global sea surface temperature analysis (Gemmill et al. 2007) is used for the filtering, with a critical temperature of 275.3 K. If the sst analysis is warmer than this, ice is removed from the ice analysis. Program seaice_filtanal

applies this filter, and performs interpolation from the hemispheric polar stereographic analyst's grids on to the global latitude-longitude grid. A version in the late 1990s had an error, which was retained in a non-operational parallel run for the Hadley Center [Rayner, personal communication 1999] as they'd developed a regression that corrected the error for their climate interests.

Grid-filling is performed by seaice_icegrid, which replaces any data gaps in the above global field with the previous day's analyzed values. In doing this, an age field is incremented for every grid point which was persisted. If the age passes 16 days, the concentration is set to zero. When instruments are performing moderately well, and data flow is not interrupted for prolonged periods (both of which were false in May, 2009) this age is seldom reached. The age limit was introduced in the 1990s because of some portions of the Antarctic which are persistently cold (hence SST filtering would not remove false ice), and have persistently heavy weather (hence false reports of ice occasionally being accepted in spite of the weather filtering). Since the action of the original weather filter is to declare points 'weather', rather than no ice, one day with a false observation could be persisted almost indefinitely through days of no data, or of weather flags. This will be reconsidered for future implementations, given the new weather filtering algorithm.

The 30' grid is produced from the 5' grid by seaice_global_reduce, by the same algorithm as used in seaice_north_reduce et al.. Given the much larger ratio in resolutions, lakes are much more extensive on the 30' grid than would be geographically faithful.

seaice_global5minxpm and seaice_globalxpm produce global graphic files as is done for the polar stereographic grids.

seaice_ice2grib produces the grib1 output of the 30' grid. Since the August 2004 implementation land has been flagged as such (1.57) in the 30' grib file. seaice_ice2grib5min produces grib1 output of the 5' grid.

The 7 October 2011 implementation added some more extensive quality control diagnostics than merely a graphic of the analysis:

seaice_monitor_c12th analyzes the 5' global grid for day to day changes in concentration (output as pushpins for changes over 20% in seaice_monitor_$PDY.kml), where PDY is the analysis date in YYYYMMDD numerical format, and bulk statistics for yesterday versus today's area and extent, variance in concentrations one day to the next, and the change in global sea ice area from day to day, output to seaice_monitor.t00z.txt. Derived from old del, delta, diff programs by way of 'all', then from ice_compare.

seaice_edge produces a very crude estimate of the northern hemisphere ice edge location. It scans the global grid at each longitude, from the pole towards the equator. The 'edge' is the latitude of the grid point where the concentration changes from nonzero (previously) to zero (in the given cell).

Web Support

grid8 – program to print out xpm files for argument-specified domains. Originated for interactive web service, but is general purpose.

Include Files

ssmi.h

include file that was intended to be general to the instrument, but, over time, incorporated ice-specific things. Eventually SDR-related code was removed.

In place by early 1994, Oldest version 22 September 1995

Change 6 March 1997 to using a variable number of orbits

Add BUFR-related functions and types 27 May 1997

Start Remove SDR-related functions and types 18 November 1998

Complete the removal, and add HIRES flag 11 October 2001

ssmiclass.h

519 noodling on a class for managing observations

520 Begun by 20 November 1998 – develop a C++ class library for working with SSMI

521 Two version now – ssmiclass.operations.h, which has many operations, but little data,
522 and ssmiclass.h, which has a working set of data declarations but few operations. The
523 latter is operational.

524 *icegrids.h*

525 declarations of grids.

526 *icessmi.h*

527 include file for seaice-specific things (vs. *ssmi.h*, which is supposed to be general about
528 the SSMI instrument/DMSP platform). It includes mapping, function declaration for
529 nasa team, weather filter limits, and prototypes for ice avg, ice_add, ice_zero, getfld,
530 newfilt, pole_fill.

531 Defines data window, minconc, nodata, weather, bad_data, coast, land.

532 Define the elements for getfld

533 typedef for ssmi, ssmi_tmp

534 In place by early 1994, oldest version on hand 22 September 1995

535 Weather flag added 20 Feb 1996 – zeroing concentrations on weather caused erroneous
536 'no ice' conditions inside the Antarctic ice pack, especially, during the melt season.

537 Regression for antenna corrections, if needed, added 1 October 1996

538 Bufr versions added 27 May 1997

539 Record data counts 18 November 1998

pole_fill generalized 20 November 1998

ice_mask added + experiments/updates to pole_fill 29 December 1999

10 October 2001 Add hiresconc, oldssmi vs. ssmi typedef polefill generalized to be pole-insensitive (arguments)

icessmi85.h

Class used in developing original high resolution sea ice concentration approach.

Not used in operations.

Had Team1 algorithm embedded.

used by:

all.C – global processing on all candidates

north.C – northern hemisphere processing on all candidates

south.C – southern hemisphere

toprocess1.C – translate from BUFR to a processing format

print85.c – print out high resolution fields

global.C – global processing

north.leastsq.C – interactive version of code for testing

glob.sh – set up graphics for the hires tests

daily.sh – run each parameter type (above codes) daily

Control Scripts + Data Files

SSMI Team 2 algorithm files

```
8 -r--r----- 1 rmg3 wd2 518 Sep 23  2005 seaice_TBthark.tab
8 -r--r----- 1 rmg3 wd2 518 Sep 23  2005 seaice_TBowark.tab
8 -r--r----- 1 rmg3 wd2 518 Sep 23  2005 seaice_TBowant.tab
8 -r--r----- 1 rmg3 wd2 518 Sep 23  2005 seaice_TBfyark.tab
8 -r--r----- 1 rmg3 wd2 518 Sep 23  2005 seaice_TBfyant.tab
8 -r--r----- 1 rmg3 wd2 518 Sep 23  2005 seaice_TBccark.tab
8 -r--r----- 1 rmg3 wd2 518 Sep 23  2005 seaice_TBccant.tab
```

AMSR-E Team2 algorithm files

```
8 -r--r----- 1 rmg3 wd2 576 Aug 11  2010 seaice_TBccark.tab.amsr
8 -r--r----- 1 rmg3 wd2 744 Aug 11  2010 seaice_TBccant.tab.amsr
8 -r--r----- 1 rmg3 wd2 744 Aug 11  2010 seaice_TBfyark.tab.amsr
8 -r--r----- 1 rmg3 wd2 744 Aug 11  2010 seaice_TBfyant.tab.amsr
8 -r--r----- 1 rmg3 wd2 599 Aug 11  2010 seaice_TBowark.tab.amsr
8 -r--r----- 1 rmg3 wd2 599 Aug 11  2010 seaice_TBowant.tab.amsr
8 -r--r----- 1 rmg3 wd2 587 Aug 11  2010 seaice_TBthark.tab.amsr
8 -r--r----- 1 rmg3 wd2 587 Aug 11  2010 seaice_TBthant.tab.amsr
```

Control Scripts

f13.jcl

date management

get satellite data

decode from satellite format

make ice concentration grids – analyst grids

filter them and make modeller grids

make grib output for ops

make graphics

distribute output

ex990.sh.sms– likewise, with addition of 'sendcom', 'senddbn' type variables for operations

*J990.sms*J-job for operations, called by SMS and calls ex script. Sets up environment variables for the ex script. Renamed to JMRF_ICEDRFT2.sms.prod

*configure*A script which attempted to do some interactive set up of directory structures and then run through data processing a la f13.jcl

*makeall.sh*Started making up scripts makeall.sh, one at each level of sorc/ directory. Each invokes either the makeall.sh at the next lower level, or the makefiles there.

Library code

In July, 1999, extracted mapxy, GRIBIT, makwmo, quedes, transt, wmoout to mmablib (**?**) rather than leave in ice concentration analysis-specific source code.

Grid corners

22 September 1995

```
Corner points on the ice maps, latitude, longitude
Latitude is negative south, longitude is negative west.

Northern hemisphere
  1,   1  25.00 -119.55
  1, 465  24.46  139.07
385,   1  24.56  -39.85
```

```
385, 465  24.02   60.33

Southern hemisphere
  1,   1 -36.90 -220.19
  1, 355 -37.80 -120.76
345,   1 -31.09 -307.14
345, 355 -31.85  -31.88
```

APPENDIX B

Additional Comments

B–1 Prehistory: Original (1994) implementations had radius of the earth as 6738, rather than 6378 km. Error found and fixed 13 September 1995.

B–2 Observation: The derived sea ice concentration is nearly the same whether one computes the ice concentration for each brightness temperature observation set in a cell and then averages those figures, or first averages the brightness temperatures and then computes a concentration from those.

B–3 Observation: The scaling of concentration is originally 0-100 (i.e. percentage cover in the cell) but was changed to 0-1 (fraction of area covered) to accord with grib standards. Archival users must currently beware of this.

B–4 Observation: The cumulative distribution of extent versus concentration, shown in figure 3, is highly nonuniform. Only 10% of the extent has concentration less than 50%, while 50% of the extent is in concentrations greater than 90%, using the CFSRR sea ice

B–5 Applying the high resolution method to 37GHz gave better results than 85GHz does. As it is only 25 km resolution itself, this was insufficient improvement for the purpose at hand.

List of Tables

TABLE 1. Availability and NCEP usage dates of satellites

Platform	Data Start	Data Cease	Used
SMMR	26 October 1978	20 August 1987	not used
SSMI F-8	9 July 1987	31 December 1991	not used
SSMI F-11	3 December 1991	30 September 1995	2/1994 - 5/1995 (pre-operational)
SSMI F-13	3 May 1995	19 November 2009	5/1995 - 11/2009
SSMI F-14		24 August 2008	8/2004 - 8/2008
SSMI F-15	15 March 2000	present	8/2004 - 5 March 2009 7 October 2011 - present
AMSR-E NASA-Aqua	19 June 2002	4 October 2011	13 May 2009 - 3 October 2011
SSMI-S F-16	not at NSIDC		not yet used
SSMI-S F-17	1 January 2007	present	19 June 2012 - present
SSMI-S F-18	not at NSIDC		not yet used
AMSR2 GCOM-W	May 2012 (launch)		not yet used

TABLE 2. Algorithms and their usage dates

Team 1 SSMI unmodified	to 8/2004
Team 1 SSMI w. NCEP modifications	to 8/2006
Team 2 SSMI w. NCEP modifications	all SSMI since (8/2006-9/2009, 10/2011-present)
Team 2 AMSRE	all AMSRE observations – 5/2009 to 10/2011
Team 1 SSMI-S	7/2012-present

TABLE 3. Quality control limits on brightness temperatures

SSMI	SSMI-S		AMSR-E		
19h	295	75	19h	305	75
19v	295	150	19v	295	150
			24h	285	100
22v	295	150	24v	285	150
37h	295	100	37h	285	100
37v	295	150	37v	285	150
85h	295	125	89h	285	135
85v	295	150	89v	285	135

List of Figures

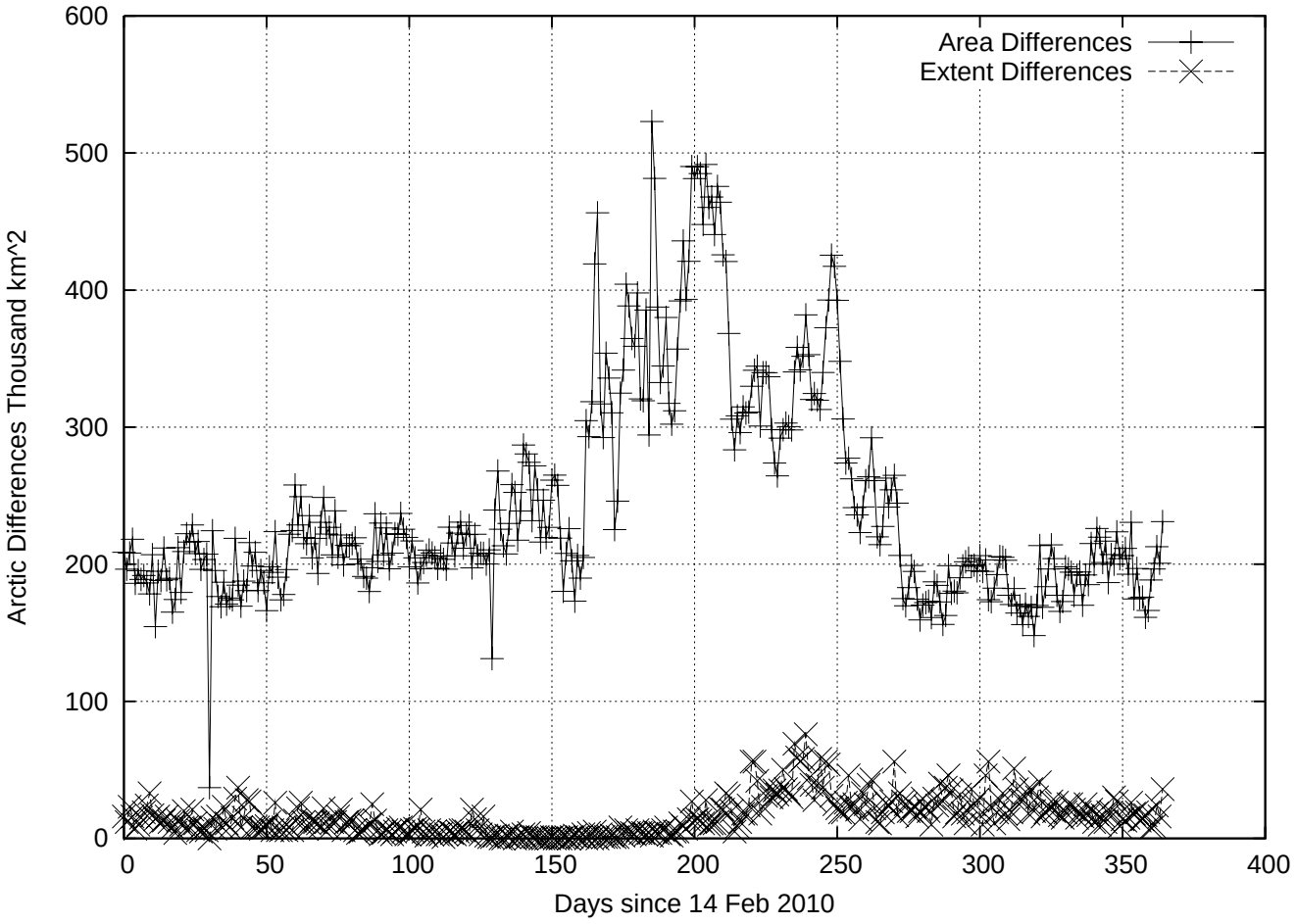

FIG. 1. Changes to Arctic Area and Extent from change to lookup table

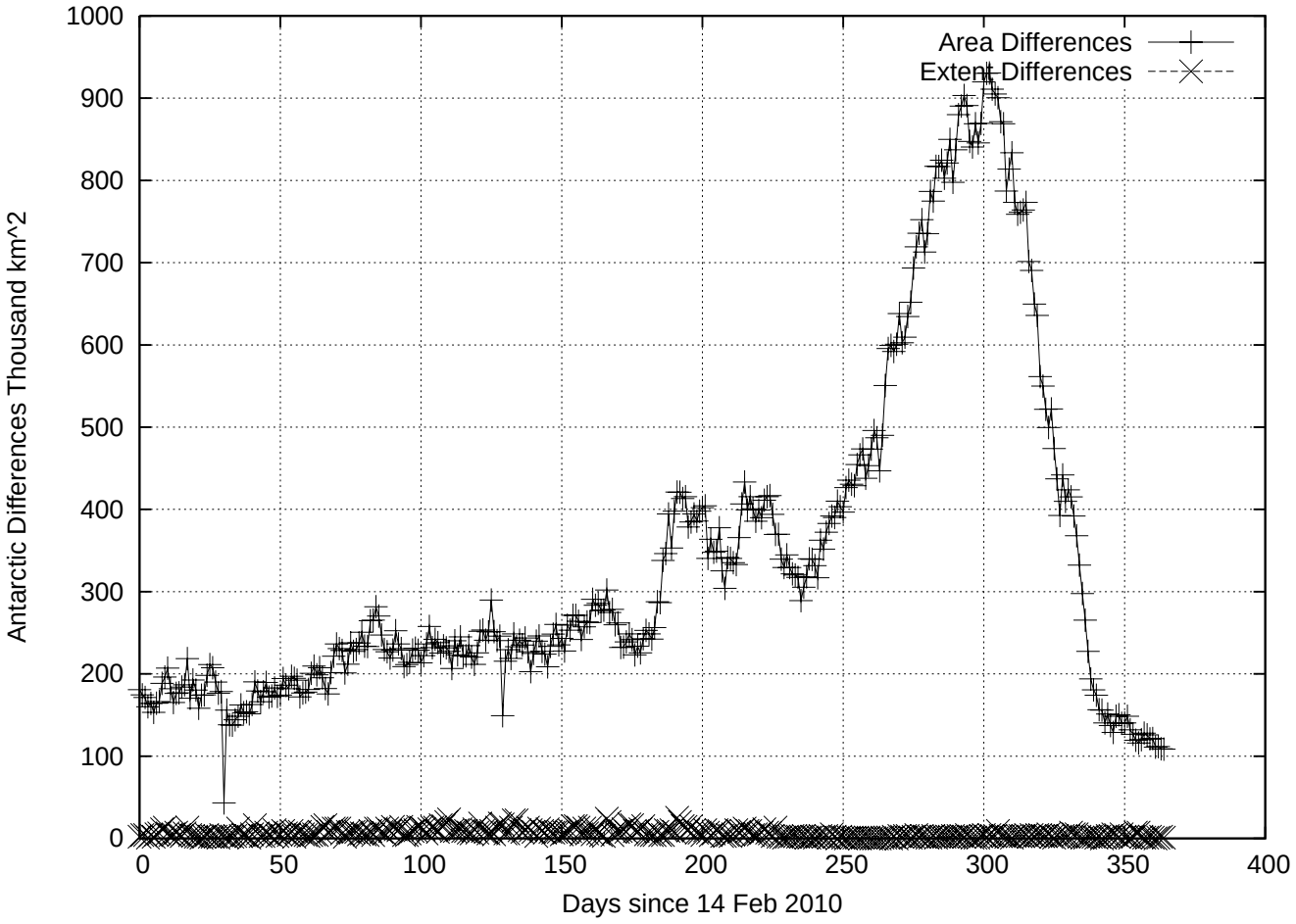

FIG. 2. Changes to Antarctic Area and Extent from change to lookup table

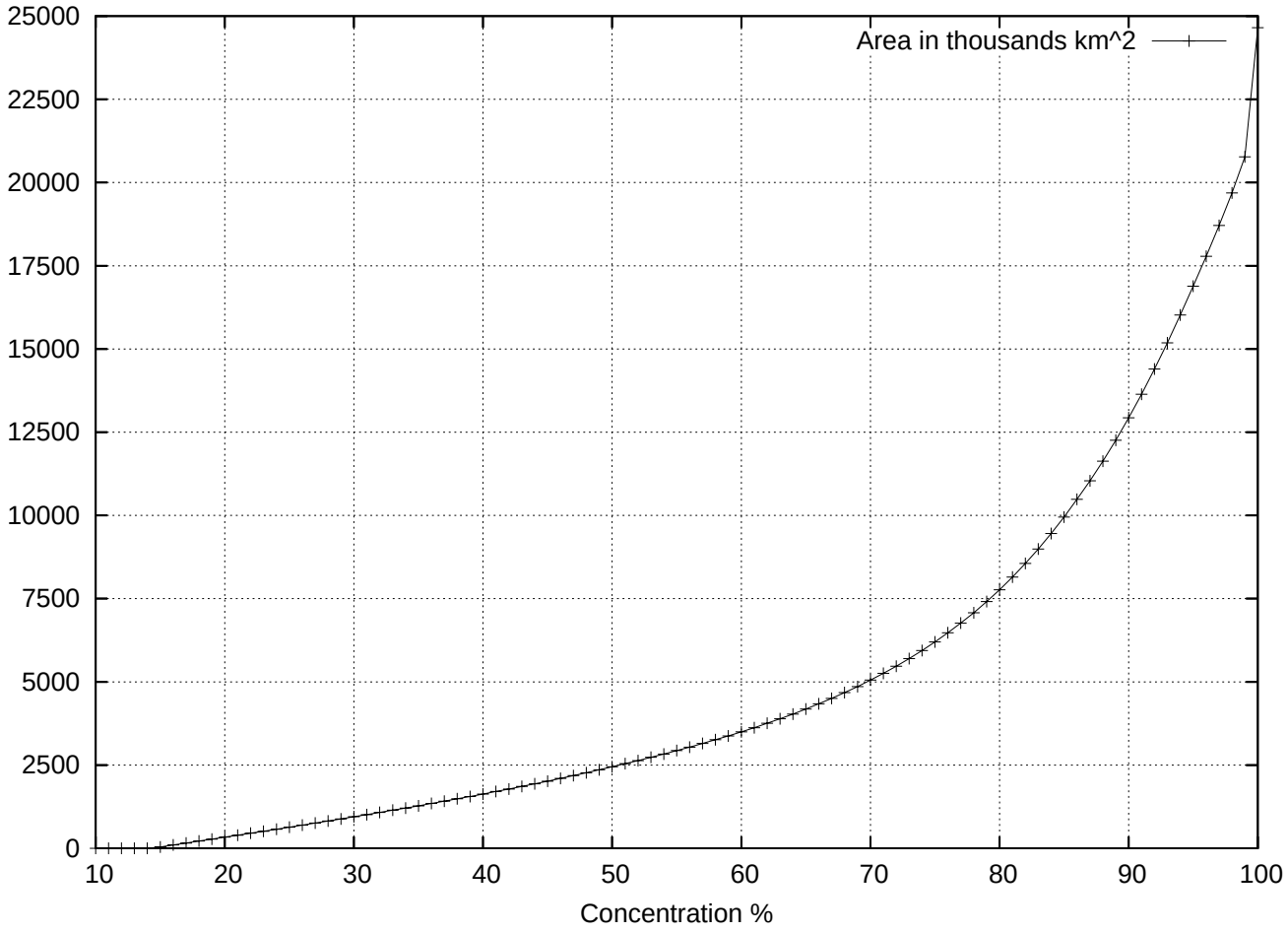

FIG. 3. Cumulative distribution function of concentrations